

Statistics of the fine structure of turbulent velocity and temperature fields measured at high Reynolds number

By **CARL H. GIBSON,**

University of California, San Diego

GILBERT R. STEGEN

Colorado State University, Fort Collins, Colorado

AND **ROBERT BRUCE WILLIAMS**

Marine Physical Laboratory, Scripps Institute of Oceanography,
La Jolla, California

(Received 25 August 1969 and in revised form 21 November 1969)

Derivatives of velocity and temperature in the wind over the ocean were found to be quite variable. Probability distribution functions of squared derivatives were consistent with lognormality predictions by Kolmogoroff, Obukhoff and Yaglom. Kurtosis values for velocity derivatives ranged from 13 to 26 and from 26 to 43 for temperature derivatives. Universal inertial subrange constants were evaluated from dissipation spectra and were found to be 40 to 300 % larger than most values reported previously. Evidence for local anisotropy of the temperature field is provided by non-zero values of the measured derivative skewness.

1. Introduction

An important property of turbulent flow is the increasing variability of the local viscous dissipation ϵ ,

$$\epsilon = \frac{\nu}{2} \left(\frac{\partial u_i}{\partial x_j} + \frac{\partial u_j}{\partial x_i} \right)^2, \quad (1)$$

as the Reynolds number of the flow increases, where ν is the viscosity, \mathbf{u} is the velocity and repeated indices in (1) are summed. Kolmogoroff's (1941) original universal similarity hypotheses did not take this variability of ϵ into account. He formed a length scale $L_K = (\nu^3/\langle\epsilon\rangle)^{\frac{1}{4}}$ and time scale $T_K = (\nu/\langle\epsilon\rangle)^{\frac{1}{2}}$ using ϵ averaged over volumes of order L , where L is the energy scale of the motion. Lauau (see Yaglom 1966) criticized Kolmogoroff's hypotheses on these grounds shortly after their publication, but it was twenty years (Kolmogoroff 1962, Obukhoff 1962) before Kolmogoroff himself suggested a refinement and extension of his hypotheses to include the random character of the dissipation. Thus, the revision of Kolmogoroff's first and second universal similarity hypotheses coincided almost exactly with their apparent experimental confirmation by a number of investigators.

It was argued that ϵ should not only be random but that its distribution should be logarithmically normal. Yaglom (1966) has shown that the assumption of a cascade process of energy transfer from very large- to very small-scale turbulent motions implies that $\ln(\epsilon)$ should be Gaussian if the transfer stages are statistically similar and independent.

The only published measurements suitable for comparison appear to be those of Gurvich (1967) who extended the assumption of dissipation lognormality to include the dissipation of temperature variance χ by thermal conduction,

$$\chi = 2\alpha(\text{grad } T)^2, \quad (2)$$

where α is the thermal diffusivity (cm^2/sec). If both χ and ϵ are lognormal, it follows that $(\Delta T)^2$ and $(\Delta u)^2$ will also be lognormal, where ΔT and Δu are temperature and velocity differences between two points separated by a distance r , $L \gg r \gg L_K$, since we expect $(\Delta T)^2 \sim \chi_r \epsilon_r^{-\frac{1}{3}} r^{\frac{2}{3}}$ and $(\Delta u)^2 \sim \epsilon_r^{\frac{2}{3}} r^{\frac{2}{3}}$ and the product of lognormal random variables is lognormal. χ_r and ϵ_r denote dissipations averaged over volumes of size r between the points of measurements of ΔT and Δu .

Gurvich (1967) measured the distribution function of ΔT for $r = 2\text{cm}$ at a height of 4 m above the ground for two records of nearly 10,000 samples. From these he used graphical methods to calculate the distribution function of $\log[(\Delta T)^2/\langle(\Delta T)^2\rangle]$, shown in figure 1 plotted on probability co-ordinates such that normal distribution functions follow straight lines. Clearly the data is well represented by straight lines, which is consistent with the lognormality of $(\Delta T)^2$. Gurvich interprets this result as experimental confirmation of the lognormal distribution of ϵ_r postulated by Kolmogoroff (1962), Obukhoff (1962) and Yaglom (1966). However, this interpretation does not seem justified for several reasons. His assumption that $(\Delta T)^2 \sim \chi_r \epsilon_r^{-\frac{1}{3}} r^{\frac{2}{3}}$ is doubtful because the separation distance of 2 cm is very close to the viscous scale $10L_K$ marking the end of the inertial subrange. Furthermore, the weak dependence of $(\Delta T)^2$ on ϵ_r will probably be dominated by the strong dependence on χ_r so the lognormality of $(\Delta T)^2$ is a better indication that χ_r is lognormal than ϵ_r . The primary motivation of the present study was to provide a more direct test of the proposed lognormality of ϵ_r by measurements of the distribution function of $(\Delta u)^2$ at very high Reynolds numbers for separation distances r much smaller than the energy scale of the turbulence L , and also to measure the distribution of the squared derivative $(du/dx)^2$ for the same reason. A more direct test of Gurvich's proposal that χ_r should be lognormal was accomplished by similar measurements of the squared temperature derivative $(dT/dx)^2$. R. W. Stewart reported similar tests of dissipation lognormality at the Boeing Turbulence Symposium, but the details of his tests are not presently available to the authors for comparison. S. Corrsin also described kurtosis measurements for wind tunnel turbulence at the Symposium.

The slope of a normal distribution function on a probability plot such as figure 1 is $1/\sigma$, where σ is the standard deviation of the random variable. From the properties of the moments of lognormal random variables (Aitchison & Brown 1957) it follows that the kurtosis K of the random variable ΔT is related to σ of $\ln(\Delta T)^2$ by

$$K = \exp(\sigma^2), \quad (3)$$

where K is defined as $\langle(\Delta T)^4\rangle/\langle(\Delta T)^2\rangle^2$. Using (3) Gurvich showed that the K value corresponding to the slope of line (a) of figure 1 is 18 compared to 3 if ΔT were Gaussian. But he also found the indicated kurtosis of line (b) is 1400. A random variable with such an extremely large kurtosis is characterized by a few large positive or negative spikes occupying a small fraction of the time.

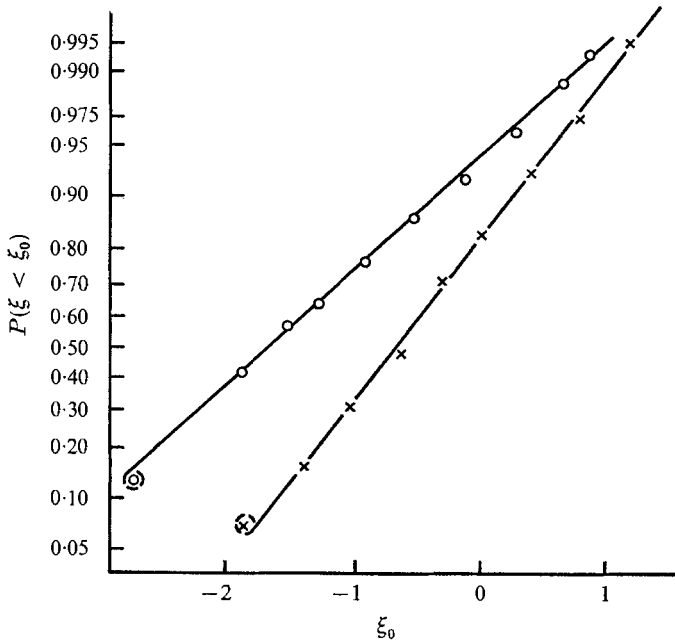


FIGURE 1. Probability distribution of the squared temperature difference compared with lognormality. $P(\xi < \xi_0)$, $\xi = (\Delta T)^2/\langle(\Delta T)^2\rangle$. \times , (a) 12 August 1965, $K = 18$ from (3); \circ , (b) 17 August 1965, $K = 1400$ from (3). Separation = 2 cm, 10^4 samples per plot (Gurvich 1967).

For comparison, if we call this fraction τ and assume the variable is one constant for the fraction τ and another constant for the fraction $1 - \tau$, the kurtosis is simply $[1/\tau(1 - \tau)] - 3 \approx 1/\tau$ for τ small compared to one. Because τ is small we see that it will be necessary to take very large sample sizes in order to measure a large kurtosis value with any statistical significance. For example, Gurvich's indicated K value of 1400 corresponds to τ of only 7×10^{-4} or about 7 samples of extreme ΔT values from his sample size of 10,000. If the $(\Delta T)^2$ distribution is indeed lognormal, then it is clear that a larger sample size will be needed to establish the parameter σ characterizing the distribution.

As already indicated, the purpose of the present paper is to describe some measurements of high Reynolds number velocity and temperature statistics, especially the distribution functions of $(\Delta u)^2$, $(dT/dx)^2$ and $(du/dx)^2$ compared to the lognormal distributions predicted for χ_r and ϵ_r . The measurements of $(\Delta u)^2$ were made over the Pacific Ocean off Mexico in March 1968 by Gibson & Williams (1969) from the Scripps Floating Instrumental Platform (FLIP). The measurements of dT/dx and du/dx were made by Gibson & Stegen in May

1969 during FLIP's participation in Project BOMEX (Barbados Oceanographic and Meteorological Experiment) in the Atlantic Ocean.

Another purpose of the BOMEX measurements was to estimate the universal inertial subrange constants for velocity and temperature spectra using dissipation rates χ and ϵ estimated from measured derivatives of T and u . Previous estimates of χ and ϵ used in the determination of the subrange constants have generally been indirect because of the difficulties of derivative measurements, and therefore subject to substantial errors. Some preliminary results of this work will be discussed. A full account will be published in the near future.

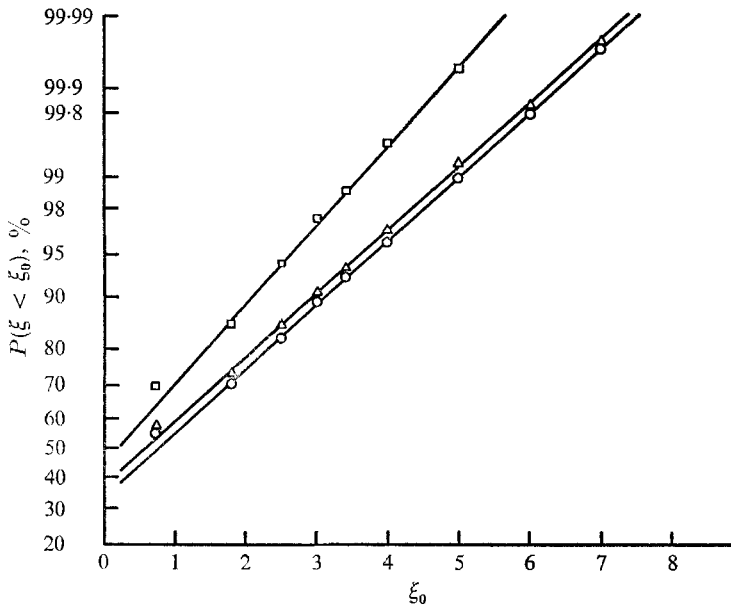


FIGURE 2. Probability distribution of the square of the velocity difference. Comparison with lognormal distribution. Separation $\Delta x = 1$ cm, 4×10^4 samples per plot (Gibson & Williams 1969). $\xi = \log_e(\Delta u)^2 + C$, $\Delta u = u(x + \Delta x) - u(x)$.

	Y (m)	Δu distribution	
		Kurtosis	Skewness
□	7	19.6	-0.52
△	2	22.1	-0.71
○	1	23.4	-0.89

2. Velocity difference measurements, Pacific Ocean

The experimental details of the Δu measurements are given elsewhere (Gibson & Williams 1969) so they need not be repeated here. The resulting probability plots of distribution functions of $\ln(\Delta u)^2$ for 1 cm separation distance measured at three heights above the ocean surface are shown in figure 2, along with calculated moments of the distributions of velocity difference Δu . The agreement of the data with straight lines is good at the higher values of $(\Delta u)^2$ indicating

qualitative support for the lognormal distribution for ϵ_r . The curvature of the data on the left is due at least in part to least count errors of the digital samples. Instrument and tape recorder noise also cause similar upward curvature distortion of the probability plot by shifting very low sample values to higher levels.

Kurtosis values calculated directly from the Δu data were all about 20, but were quite different from K values inferred from the slopes of the straight lines in figure 2. The data for height 7 m indicates K should be about 15, but for 1 and 2 m the slope implies kurtosis values of about 37. These large K values are in conflict not only with the values measured directly, but also with Kolmogoroff's prediction that intermittency should increase with Reynolds number. Because of the sensitivity of the probability plot to the effects of noise, K values inferred from plot slopes using (3) assuming $(\Delta u)^2$ is lognormal are inaccurate compared to values calculated from Δu samples.

Another quantity calculated from the Δu samples is the skewness S , defined as the mean cube divided by the $\frac{3}{2}$ power of the mean square $\langle(\Delta u)^3\rangle/\langle(\Delta u)^2\rangle^{\frac{3}{2}}$. According to local isotropy theory (taking Δu for 1 cm as a measure of the derivative) this quantity should be constant and proportion to mean principal rate of strain product $\langle\alpha\beta\gamma\rangle$, where $e_{ij} = (\partial u_i/\partial x_j + \partial u_j/\partial x_i)/2$ is the rate of strain tensor with principal values $\alpha \geq \beta \geq \gamma$. Since by continuity $\alpha + \beta + \gamma = 0$, γ must be negative and α positive, so the sign of S determines the sign of β . Since all S values are negative, it appears that fluid elements usually have two positive principal strain rates; that is, they tend to be flattened out into sheets. The measured values around -0.7 are consistent in sign but larger in magnitude than a limit of -0.3 inferred by Batchelor (1953) from measurements of Townsend & Stewart (1951) and universal equilibrium theory. Gurvich (1960) has also measured S for separation distances of 25 and 50 cm. His values were smaller in magnitude but also negative, ranging from -0.19 to -0.62 .

3. Derivative measurements, Atlantic Ocean

3.1. Experimental arrangements

Measurements of velocity and temperature fluctuations were made at heights between 2 and 12 m above the mean ocean surface. The temperature and velocity sensors were mounted on an automatic positioning device developed by R. Fleagle at the University of Washington. This device cycled the probe support between stations nominally at 12, 8, 4 and 2 m above the surface, stopping for 45 sec measurement periods at each station. The probe support moved along a track on a vertical boom mounted 50 ft. to the side of FLIP, in order to minimize the distortion of the wind profile by the ship. The streamwise velocity fluctuations were measured using a linearized constant resistance anemometer (Thermo-Systems Model 1054A). The sensor was a 3.8μ diameter wire 1.25 mm long. The bridge was operated with a wire overheat of 1.45 and the linearizer zeroed with the wire shielded (operating temperature $\approx 130^\circ\text{C}$). At this operating temperature, the low level temperature fluctuations in the flow had a negligible influence on the velocity measurements. The use of very

long cables to the sensor (≈ 40 m), posed a problem with regard to stable operation of the anemometer bridge circuit. However, careful adjustment of the bridge parameters resulted in stable operation with a frequency response in excess of 5 KHz. A continuous velocity calibration signal was provided by a sensitive 3-cup anemometer (Beckman-Whitley—calibrated by the Bureau of Standards) mounted 30 cm below the hot-wire probe. The voltage signals from the hot-wire and cup anemometers were simultaneously recorded on an FM tape recorder. Later, the digitally sampled data were averaged over 10 sec intervals. By plotting a number of such averages, the calibration curve was generated. The curve was linear with less than $\pm 2\%$ scatter over a 2:1 range in velocity, and the extrapolated straight line passed through zero.

Temperature fluctuations were detected using cold-wire thermometer techniques. The sensor was an extremely fine (and fragile!) platinum wire, $0.6\ \mu$ diameter and 2 mm long mounted 5 cm above the anemometer sensor. Temperature fluctuations in the wire were detected using an a.c. bridge with a phase-sensitive demodulator. The frequency response of the temperature sensing system was limited by the thermal response time of the sensor to about 2 KHz. The a.c. bridge was arranged to give a maximum sensor current of about 1 mA, a value sufficiently low to ensure negligible velocity sensitivity.

Very little change was observed in the temperature signal during movement between vertical stations despite significant vibrations in the support device, indicating negligible sensitivity to velocity and strain gauge effects during steady operation. The temperature system was calibrated by introducing step changes in resistance with a precision decade resistance box placed in the known arm of the 1:1 a.c. bridge.

Before recording, the velocity and temperature signals were preconditioned with various analogue circuits. The anemometer signal was first band-pass filtered between 2 Hz and 2 KHz with active filters (attenuation = 24 db/octave). The signal was then amplified to a value compatible with the tape recorder (± 1.4 V) and finally recorded. The amplified signal was also electronically differentiated and recorded. The differentiator had a time constant of 0.5 msec, with a measured phase shift error of 15° at 500 Hz.

The output of the a.c. bridge was recorded directly. To obtain a differentiated temperature signal, the a.c. bridge signal was first low-pass filtered at 2 KHz with an active filter (attenuation = 24 db/octave). The differentiator had a time constant of 0.5 msec, with a measured phase shift error of 3° at 500 Hz. The differentiated temperature signal had to be slightly attenuated for compatibility with the tape recorder.

A 7-channel FM tape recorder (Ampex SP-300) was used to record the various signals. At the recording speed of $7\frac{1}{2}$ in./sec, the frequency response extended to 2.5 KHz, with a signal-to-noise ratio of 35 db. One channel of the recorder was used to record a probe position signal. This signal was shorted when the probe was stopped, so that it could be used for flutter compensation if needed. The tape recorder was calibrated by recording a precision triangle function and a short on each channel before and after each period of data recording.

The analogue tapes were played back and converted to digital form in the

laboratory. At each height the data was broken up into 50 records containing 2048 12-bit samples per record. This gives the spectra at each height 100 statistical degrees of freedom. The sampling rate was 2085 Hz, so each record represents almost one second of data. Ten records were obtained in sequence during each of five different 45 sec sampling periods at the particular height in order to make up the files of 50 records. Each cycle through the four heights took about 3 min, so the data is a representative sample of about 20 min of data collection. Before digital sampling, an analogue low-pass filter set at 1 KHz (about one-half the sampling rate) was used to prevent aliasing of the spectra.

Reviewing the reduced data, the maximum frequency distinguishable from the noise was about 1 KHz. Examining the electronics, we see that the system frequency response was limited by the low-pass filter used to prevent aliasing of the spectra. At the corner frequency (1 KHz) the dissipation spectra has fallen by three decades. Under similar circumstances, Stegen (1969) has shown that the phase errors introduced by limited system response have negligible influence on the higher order statistics. However, it was necessary to correct the spectra above 500 Hz for the filter response. These corrections made less than 10% change in the measured universal constants.

3.2. Results

A summary of the conditions of measurement as well as the various calculated statistical quantities for the temperature and velocity fluctuations measured in the Atlantic Ocean during BOMEX is given in table 1. The turbulent boundary layer was nearly neutral, with sea-surface temperature (bucket) only 0.3°C warmer than the air at 8 m. Measurements were made in the afternoon following a long period of steady light wind from the east characteristic of Caribbean trade winds in early May.

Height <i>y</i> (m)	$\langle u \rangle$ (m/sec)	<i>Re</i> $\times 10^6$	$\left\langle \left(\frac{du}{dx} \right)^2 \right\rangle$ (sec ⁻²)	<i>S</i> $\left(\frac{du}{dx} \right)$	<i>K</i> $\left(\frac{du}{dx} \right)$	$\left\langle \left(\frac{dT}{dx} \right)^2 \right\rangle$ (°C ² /m ²)	<i>S</i> $\left(\frac{dT}{dx} \right)$	<i>K</i> $\left(\frac{dT}{dx} \right)$
12.25	5.20	4.1	4.2	-0.85	26	0.216	-0.40	43
8.25	4.96	2.7	12.1	-0.81	20	0.547	-0.72	38
4.25	4.76	1.3	19.3	-0.44	13	0.839	-0.48	37
2.25	4.63	0.7	29.0	-0.72	15	1.817	-0.72	25

Time: 3.00 p.m., 6 May 1969.

Position: 14°30' N, 58°30' W. Atlantic.

Re = Reynolds number $\langle u \rangle y / \nu$, ν = kinematic viscosity of air.

T_{air} = 28.0°C, T_{sea} = 28.3°C, *K* = kurtosis, *S* = skewness.

TABLE 1. Summary of conditions and results

Figure 3 shows the dissipation spectrum of the streamwise velocity $k_1^2 \Phi(k_1)$ measured from the derivative at a mean height of 2.25 m above the water, where $\Phi(k_1)$ is the one-dimensional spectrum such that

$$\int_0^\infty \Phi(k_1) dk_1 = \langle u'^2 \rangle$$

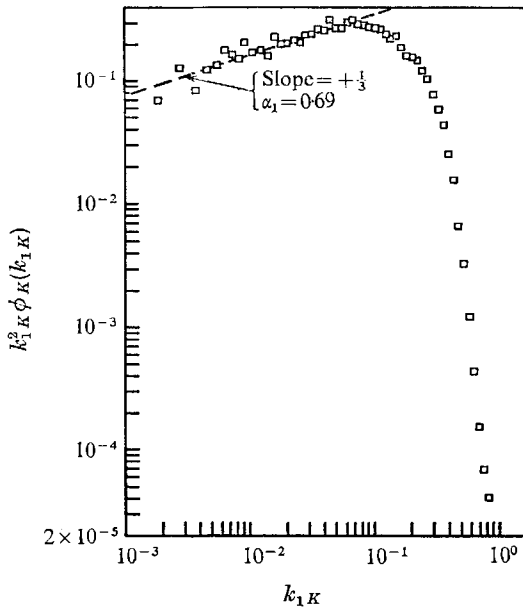


FIGURE 3. Velocity derivative spectrum normalized with Kolmogoroff scales. 10^5 samples. Height = 225 cm, $\langle u \rangle = 463$ cm/sec, $\langle \epsilon \rangle = 68$ cm²/sec³.

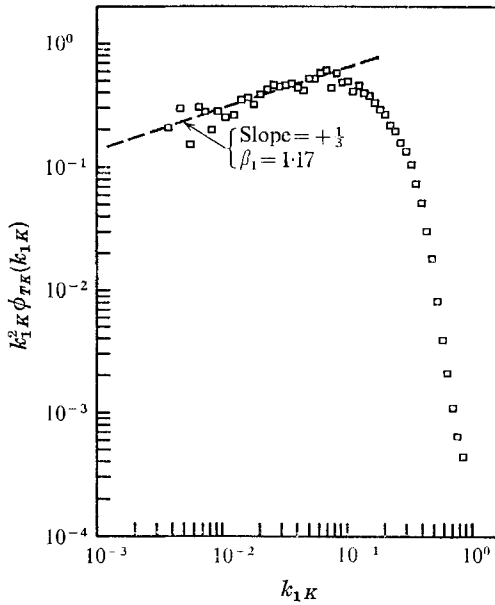


FIGURE 4. Temperature derivative spectrum normalized with Kolmogoroff scales. 10^5 samples. Height = 225 cm, $\langle u \rangle = 463$ cm/sec, $\langle \epsilon \rangle = 68$ cm²/sec³, $\langle \chi \rangle = 2.40 \times 10^4$ °C²/sec.

and u' is the fluctuating component of velocity in the streamwise x_1 direction. The spectrum and wave-number k_1 have been normalized with Kolmogoroff length and time scales L_K and T_K , defined above. The mean dissipation $\langle \epsilon \rangle$ was estimated from the derivative of the velocity du_1/dx_1 assuming local isotropy using the relation

$$\langle \epsilon \rangle = 15\nu \left\langle \left(\frac{du_1}{dx_1} \right)^2 \right\rangle \doteq 15\nu \frac{1}{\langle u_1 \rangle^2} \left\langle \left(\frac{du_1}{dt} \right)^2 \right\rangle, \quad (4)$$

where Taylor's hypothesis was used to convert measured time derivatives to space derivatives in the usual way. An unusually large value of the Kolmogoroff inertial subrange constant $\alpha_1 = 0.69$ is indicated by the data of figure 3, where α_1 is defined by $\Phi = \alpha_1 \langle \epsilon \rangle^{\frac{2}{3}} k_1^{-\frac{5}{3}}$.

Figure 4 shows the dissipation spectrum of the temperature field $k_1^2 \Phi_T(k_1)$, normalized with $\langle \epsilon \rangle$, ν and $\langle \chi \rangle$, where $\langle \chi \rangle$ was estimated from

$$\langle \chi \rangle = 6D \left\langle \left(\frac{dT}{dx_1} \right)^2 \right\rangle \doteq 6D \frac{1}{\langle u_1 \rangle^2} \left\langle \left(\frac{dT}{dt} \right)^2 \right\rangle, \quad (5)$$

assuming local isotropy of the temperature field and again using Taylor's hypothesis to convert time to space. In this case the inertial subrange constant β_1 , defined by

$$\Phi_T = \beta_1 \langle \chi \rangle \langle \epsilon \rangle^{-\frac{1}{3}} k_1^{-\frac{5}{3}}, \quad \text{where} \quad \int_0^\infty \Phi_T dk_1 = \langle T'^2 \rangle,$$

is found to be 1.17, where T' is the fluctuating component of the temperature T . This value is much larger than β_1 values previously reported. For example, Gibson & Schwarz (1963) found β_1 values of only 0.33 to 0.44, and Grant *et al.* (1968) report $\beta_1 = 0.31 \pm 0.06$.†

Two factors which might account for part of this dramatic increase in β_1 are described below: first, anisotropy of the temperature fine structure may result in mean shift of horizontal temperature gradients toward the vertical due to the mean strain of the shear layer; and secondly, the very large intermittency of the velocity dissipation may reduce the effective least principal strain rate which dominates the generation of the fine structure of scalar fields.

3.2.1. *Effect of anisotropy on temperature spectrum.* If the temperature field were locally isotropic, statistical descriptions of the temperature derivative such as the skewness

$$S \equiv \left\langle \left(\frac{dT}{dx} \right)^3 \right\rangle / \left\langle \left(\frac{dT}{dx} \right)^2 \right\rangle^{\frac{3}{2}}$$

would be invariant to rotations and reflexions of the co-ordinate axes. Therefore, reflecting co-ordinate x to $x' = -x$ gives $S = -S'$; hence, S must be identically zero. But the present measurements of $S(dT/dx)$ show (table 1) that it is consistently positive with some tendency to increase close to the surface, even though the kurtosis shows a corresponding decrease. Thus we see that the fine structure of the temperature field cannot be locally isotropic. It also seems

† Yaglom reports (private communication) precise agreement of these values with corrected values of β_1 obtained by Tevang, Gurvich, Zubkovskii & Meleshkin.

that the tendency toward local isotropy with increasing Reynolds number $\langle u \rangle y / \nu$ is rather weak, since the skewness shows little or no decrease going from height 2.25 to 12.25 m despite a factor of six increase in Reynolds number.

If the temperature derivative is anisotropic there may be an effect on the inertial subrange constant β_1 measured assuming local isotropy. If the field is stretched so that the local gradient vectors are more vertical on the average, then the horizontal wave-number marking the diffusive cut-off k_{1c} will be reduced to some lower value $k'_{1c} < k_{1c}$. But from (5)

$$6D \int_0^\infty k_1^2 \Phi_T dk_1 \equiv \chi,$$

assuming local isotropy of the T field. In normalized form

$$\int_0^\infty k_{1K}^2 \Phi_{TK} dk_{1K} = \nu/6D.$$

Now if (for the sake of argument) we assume $\Phi_{TK} = \beta_1 k_{1K}^{-5/3}$ for $k_{1K} < k_{1c}$ and $\Phi_{TK} = 0$ for $k_{1K} > k_{1c}$, we find

$$\beta_1 = \frac{2}{9} (\nu/D) k_{1c}^{-4/3}.$$

Therefore, since k'_{1c} for the assumed anisotropy is less than k_{1c} for the isotropic case, we can conclude that

$$\beta'_1 > \beta_1$$

for enhanced vertical gradients. The mean strain of the boundary layer is such that we might expect fluid elements to be stretched into horizontal sheets, therefore tending to enhance the vertical and decrease the horizontal streamwise temperature gradients.

3.2.2. *Effect of ϵ intermittency on temperature spectrum.* Batchelor (1959) has shown that the finest structure of weakly diffusive scalar fields mixed by turbulence is determined by the local rate of strain. The smallest scale fluctuation, corresponding to the length scale of the diffusive cut-off of the scalar spectrum, is given by the 'Batchelor length scale' $L_B = (D/\gamma)^{1/2}$, where the strain parameter γ is normally taken to be $(\epsilon/\nu)^{1/2}$. Batchelor's analysis was extended by Gibson (1968*a*), who concludes that the finest structure of all scalar fields should be determined by the local strain rate, independent of the 'Prandtl' number ν/D .

Gibson (1968*b*) also suggested that the diffusive cut-off length scale would increase if the turbulence is strongly intermittent (following a comment of B. Hughes) because the local strain magnitude follows the mean root dissipation rather than the root mean. Thus, if we assume the diffusive cut-off is $(D/\gamma_{\text{eff}})^{1/2}$, where

$$\gamma_{\text{eff}} = \langle +(\epsilon/\nu)^{1/2} \rangle = \langle \epsilon/\nu \rangle^{1/2} \frac{\langle +(\epsilon)^{1/2} \rangle}{\langle \epsilon \rangle^{1/2}} = \gamma/I$$

and the 'intermittency factor' I is defined as the root mean to mean root dissipation ratio, then $(D/\gamma_{\text{eff}})^{1/2} = L_B \sqrt{I}$. Since $I \geq 1$ by Schwartz's inequality we conclude the effect of intermittency will always be to increase the length scale marking the diffusive cut-off.

The coefficient β_1 will also be affected by I . Following the previous sharp cut-off spectrum model used in the discussion of the effect of anisotropy, we find $(\beta_1)_I = \beta_1 I^{\frac{2}{3}}$. The quantity I has not yet been measured. Approximating I by $\sqrt{(\frac{1}{3}K)}$ to obtain a crude measure of the intermittency effect on β_1 gives $(\beta_1)_I = \beta_1 (\frac{1}{3}K)^{\frac{1}{3}}$, so we expect β_1 to increase with increasing intermittency. Since K ranged from 13 to 26 for the present measurements, the factor $\frac{1}{3}K^{\frac{1}{3}}$ ranges from 1.7 to 2.1. This factor is not large enough to account for the observed increase in β_1 by a factor of about 3 above the low Reynolds number measurements, but it is in the right direction, and may have been underestimated by the approximations. However, it is in conflict with the Grant *et al.* (1968) ocean measurements which were also at high Reynolds numbers and presumably comparably high levels of intermittency, yet gave results considerably lower than obtained here. It is clear that further measurements of β_1 both at low and high Reynolds numbers are needed to resolve these large apparently experimental inconsistencies.

3.2.3. *Distribution functions of derivatives.* Both velocity and temperature derivatives are quite spikey when observed on an oscilloscope, especially the temperature. This non-Gaussian behaviour is clearly illustrated by the probability plot of the distribution functions of temperature and velocity derivatives normalized by standard deviations shown in figure 5. No portion of the two S-shaped curves approaches a straight line characteristic of a normal distribution function. Negative velocity derivative distribution was plotted so both skewness values have the same sign for the two distributions.

Figure 6 shows probability plots of the distribution functions for the logarithm of the squared velocity derivatives measured at the four heights from 2 to 12 m up. The derivative square is normalized by the derivative variance. Also shown with each distribution function is a straight line with slope corresponding to the calculated kurtosis of the derivative using (3). Values of K ranged from 13 to 26. Agreement of the data points with the calculated straight lines is very good, at least for the upper four or five powers of e , which is all that can be expected given the signal to noise ratio of the tape recorder of only about 35 db corresponding to $\Delta\xi_0 = 4$ in figure 6.

Curvature of the data points above the straight lines (corresponding to lognormality) is certainly due to noise at the lowest probability values, and may possibly account for all departure from lognormality observed. The estimates of the probability for high derivative magnitudes are not affected by noise and are consistent with lognormality. Estimates of probability for low derivative magnitudes are dominated by noise, and it is not possible to say that a departure from lognormality was observed based on the measurements of figure 6 and the known system noise levels. Indeed, to extend the measured probability functions to 20% would require an overall system signal to noise ratio of better than 70 db. Note that the effect of noise on the distribution function is to reduce the slope, which implies a larger kurtosis for du/dx than was actually measured.

Figure 6 also shows calculated values of skewness S . As determined previously for Δu (1 cm) in figure 2 the skewness values were large and negative, ranging from -0.4 to -0.9 .

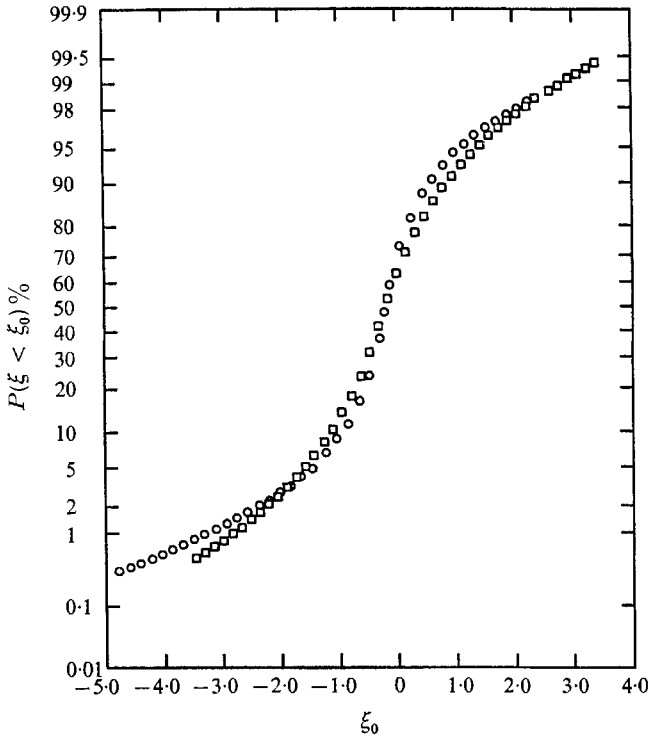


FIGURE 5. Probability distribution of temperature and velocity derivatives compared with Gaussian. Height = 225 cm, 10^5 samples per plot. \circ , $\xi = (dT/dx)/\langle (dT/dx)^2 \rangle^{1/2}$; \square , $\xi = -(du/dx)/\langle (du/dx)^2 \rangle^{1/2}$.

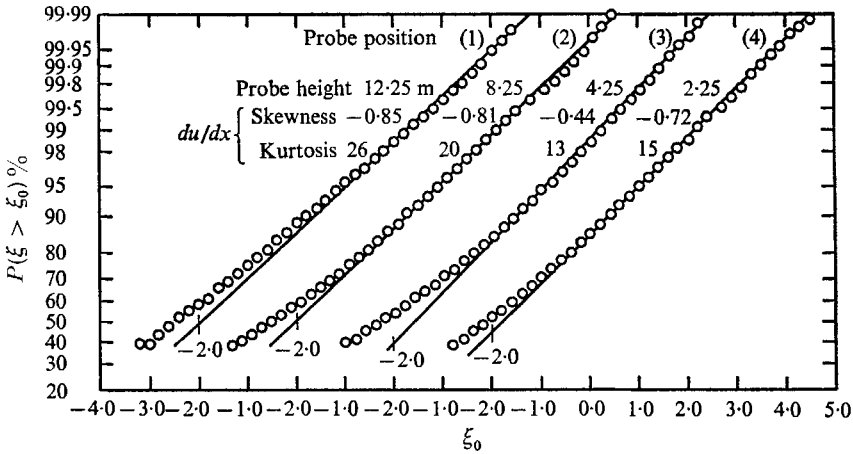


FIGURE 6. Probability distributions of squared velocity derivative compared with lognormality. 10^5 samples per plot. $\xi = \ln[(du/dx)^2/\langle (du/dx)^2 \rangle]$.

Figure 7 shows a similar comparison of the temperature derivative squared with lognormality as suggested by Gurvich. Agreement with the straight lines calculated from the measured kurtosis does not extend to as low a probability as for the velocity derivatives in figure 6, due to the lower signal/noise ratio for the temperature derivative. Kurtosis values are larger for temperature than for velocity, ranging from 26 to 43, but are not nearly as large as the value of 1400 inferred by Gurvich from his measured probability plot in figure 1. Straight lines fitted to the lower portions of the probability plots of figure 7 also indicate very large K values, as high as 8000 for position (4), but the slopes are almost certainly due to noise.

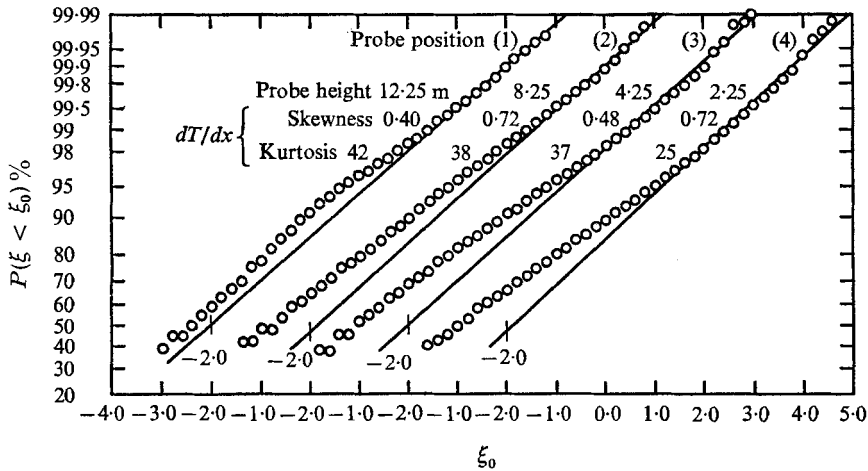


FIGURE 7. Probability distributions of squared temperature derivative compared with lognormality. 10^5 samples per plot. $\xi = \ln[(dT/dx)^2 / \langle (dT/dx) \rangle]$.

4. Summary and discussion

Derivatives of high Reynolds number velocity and temperature fluctuations were measured in the atmospheric boundary layer over the open ocean. Probability distribution functions were calculated and found to be highly non-Gaussian. Non-zero values of temperature gradient skewness were found, indicating some local anisotropy for the temperature field. Kurtosis values were also very large, increasing from 15 to 27 with height from 2 to 12 m for the streamwise velocity derivative, and increasing from 26 to 43 for the temperature derivative.

Probability distribution functions were calculated for the squared derivatives and compared with the prediction of Kolmogoroff, Obukhoff and Yaglom that the viscous and diffusive dissipation rates should be lognormal. Portions of the measured distribution functions not affected by noise were found to be in good agreement with lognormality. Kurtosis values of the derivatives calculated from the squared derivative distributions assuming lognormality were also in good agreement with the kurtosis values actually measured.

One-dimensional spectrum functions were calculated from velocity and temperature signals, and these were normalized by Kolmogoroff length, time and scalar scales calculated from molecular diffusivities of momentum and heat, as well as viscous and diffusive dissipation rates calculated from the derivatives assuming local isotropy.

Universal inertial subrange constants calculated from the derivative spectra at the point closest to the ocean surface were found to be much larger than most values previously reported in the literature. The one-dimensional velocity constant α_1 was found to be 0.69 at a mean height of 2.25 m above the surface, compared to usual values of only about 0.5. The one-dimensional scalar constant β_1 was found to be 1.17, which is 3 to 4 times larger than values previously reported.† It was shown that such large values can at least partially be explained by assuming local gradients are anisotropic in the same direction as the mean gradients. However, preliminary measurements of β_1 from this study at the upper levels (to be published) at larger Reynolds numbers and less shear only show a decrease to about 1.0. It was also shown that intermittency effects might increase β_1 considerably. Gibson (1968*b*) has shown that Batchelor's cut-off function implies that β_1 values should be about 0.9 neglecting intermittency effects and assuming the tendency of turbulent fluid particles is to be stretched into sheets. Whether any or all of these effects are active remains to be seen.

The large measured values of α_1 are more difficult to understand. Part of the increase may be due to local anisotropy effects as suggested for the scalar spectrum, but Pond *et al.* (1966) report $\alpha_1 = 0.48 \pm 0.055$ from measurements made under similar conditions of shear and presumably with similar anisotropy effects. At larger heights in the profile, preliminary values of α_1 only seem to decrease to about 0.6. The only published results indicating such large values of α_1 are those of Kistler & Vrebalovich (1966) whose spectra indicate α_1 values of 0.65 in very high Reynolds number grid turbulence. Unfortunately the Co-Op Wind Tunnel was dismantled before the results could be confirmed. Most recently, the results of Sheih (1969) measured in the atmosphere at high Reynolds number indicate a value of $\alpha_1 = 0.59$.

Kraichnan (1968) derived $\alpha_1 = 0.58$ using the abridged Lagrangian History Direct Interaction approximation. Pao (1965) also obtained a relatively large value of $\alpha_1 = 0.55$ by fitting his spectral cut-off function to measured viscous cut-off shapes with α_1 as the adjustable parameter. Clearly further careful measurements of this important quantity are needed in order to establish whether it is indeed a universal constant of high Reynolds number turbulence. If it is not an absolute constant, then it should be established how and why it varies.

The authors' spectral analysis, calibrations and calculations of α_1 , β_1 , ϵ and χ were repeated completely by Carl Friche using the data tapes and an IBM 1130 computer, and the refined results are reported here. Filter corrections resulted in substantial changes in ϵ and χ values, although compensating errors resulted

† Similarly large values of β_1 have also recently been observed by Noel Boston over a mud flat (private communications from N. Boston and R. W. Stewart).

in virtually no change in values of α_1 and β_1 . Note that the value of ϵ given in figure 3 corresponds to a 10 metre drag coefficient $C_{10} = 1.6 \times 10^{-3}$ (Gibson & Williams 1969), which is close to the expected value.

The authors would like to acknowledge the valuable assistance of Steve McConnell, S. M. Bhogte and Ian Hirschsohn in reducing the data, and particularly the co-operation of R. Fleagle and Clayton Paulson of the University of Washington in allowing us to mount probes on their positioning device.

Financial support was provided primarily by NONR Contract no. 2216(23) and Project THEMIS Contract no. F44620-68-C-0010 and partially by ARPA Contract no. DA-31-124-ARO-D-257 and NSF Contract no. GH 24.

REFERENCES

- AITCHISON, J. & BROWN, J. A. C. 1957 *The Lognormal Distribution*. Cambridge University Press.
- BATCHELOR, G. K. 1953 *The Theory of Homogeneous Turbulence*. Cambridge University Press.
- BATCHELOR, G. K. 1959 *J. Fluid Mech.* **5**, 113.
- GIBSON, C. H. 1968*a* *Phys. Fluids*, **11**, 2305.
- GIBSON, C. H. 1968*b* *Phys. Fluids*, **11**, 2316.
- GIBSON, C. H. & SCHWARZ, W. H. 1963 *J. Fluid Mech.* **16**, 365.
- GIBSON, C. H. & WILLIAMS, R. B. 1969 *Proceedings AGARD Specialists Symposium on the Aerodynamics of Atmospheric Shear Flows*. Munich: AGARD CP no. 48.
- GRANT, H. L., HUGHES, B. A., VOGEL, W. M. & MOILLIET, A. 1968 *J. Fluid Mech.* **34**, 423.
- GURVICH, A. S. 1960 *Dokl. AN SSSR*, **134**, 1073.
- GURVICH, A. S. 1967 *Dokl. AN SSSR*, **172**, 554.
- KISTLER, A. L. & VREBALOVICH, T. 1966 *J. Fluid Mech.* **26**, 37.
- KOLMOGOROFF, A. N. 1941 *Dokl. AN SSSR*, **30**, 301.
- KOLMOGOROFF, A. N. 1962 *J. Fluid Mech.* **13**, 82.
- KRAICHNAN, R. H. 1968 *Phys. Fluids*, **11**, 945.
- OBUKHOFF, A. M. 1962 *J. Fluid Mech.* **13**, 77.
- PAO, Y. H. 1965 *Phys. Fluids*, **8**, 1063.
- POND, S., SMITH, S. D., HAMBLIN, P. F. & BURLING, R. W. 1966 *J. Atm. Sci.* **23**, 376.
- SHIEH, C. M. 1969 Dissertation, The Penn. State Univ.
- STEGEN, G. R. 1969 *Phys. Fluids*, **12**, 723.
- YAGLOM, A. M. 1966 *Dokl. AN SSSR*, **166**, 49.